

Negative vortices: The formation of vortex rings with reversed rotation in viscoelastic liquids

Carlos Palacios-Morales, Christophe Barbosa, Francisco Solorio, and Roberto Zenit

Citation: *Physics of Fluids* **27**, 051703 (2015); doi: 10.1063/1.4919949

View online: <http://dx.doi.org/10.1063/1.4919949>

View Table of Contents: <http://scitation.aip.org/content/aip/journal/pof2/27/5?ver=pdfcov>

Published by the [AIP Publishing](#)

Articles you may be interested in

[Vortex ring formation in oscillatory pipe flow of wormlike micellar solutions](#)

J. Rheol. **58**, 149 (2014); 10.1122/1.4851316

[Viscoelastic flow in a 3D square/square contraction: Visualizations and simulations](#)

J. Rheol. **52**, 1347 (2008); 10.1122/1.2982514

[Vortex shedding in confined swirling flow of polymer solutions](#)

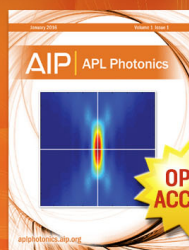
Phys. Fluids **19**, 023103 (2007); 10.1063/1.2709705

[Effect of time-dependent piston velocity program on vortex ring formation in a piston/cylinder arrangement](#)

Phys. Fluids **18**, 033601 (2006); 10.1063/1.2188918

[Confined flow vortex breakdown control using a small rotating disk](#)

Phys. Fluids **16**, 4750 (2004); 10.1063/1.1813061



Launching in 2016!
The future of applied photonics research is here

AIP | APL
Photonics

Negative vortices: The formation of vortex rings with reversed rotation in viscoelastic liquids

Carlos Palacios-Morales,¹ Christophe Barbosa,² Francisco Solorio,¹ and Roberto Zenit²

¹*Departamento de Termodinámicos, Facultad de Ingeniería, Universidad Nacional Autónoma de México, Av. Universidad 3000, México D.F. 04510, México*

²*Instituto de Investigaciones en Materiales, Universidad Nacional Autónoma de México, México D.F. 04510, México*

(Received 23 December 2014; accepted 2 April 2015; published online 15 May 2015)

The formation process of vortex rings in a viscoelastic liquid is studied experimentally considering a piston-cylinder arrangement. Initially, a vortex ring begins to form as fluid is injected from the cylinder into the tank in a manner similar to that observed for Newtonian liquids. For later times, when the piston ceases its motion, the flow changes dramatically. A secondary vortex with reversed spinning direction appears and grows to be as large in size as the original one. The formation process is studied by contrasting the evolution with that obtained for Newtonian liquids with equivalent Reynolds numbers and stroke ratios. We argue that the reversing flow, or negative vortex, results from the combined action of shear and extension rates produced during the vortex formation, in a process similar to that observed behind ascending bubbles and falling spheres in viscoelastic media. © 2015 AIP Publishing LLC. [<http://dx.doi.org/10.1063/1.4919949>]

Vortex rings are fluid structures which have been studied extensively¹ due to their prevalence in many natural phenomena and engineering applications. They can be readily observed during outflow of starting jets such as those in automobile exhaust systems² and outburst volcanoes³. A wide variety of engineering applications uses vortical properties in innovative design such as fire extinguishing,⁴ submarine propulsion,^{5,6} weaponry,⁷ and even umbrellas.⁸

For the particular case of biological flows, some researchers have shown that the formation of vortex rings is very important in the efficiency of propulsion of some aquatic animals.^{9–11} The circulation of the vortex rings that are produced as the blood passes through heart valves has been proposed as a measure of the heart performance.¹² It is important to point out that in many biological flows, and also numerous industrial applications, the fluids have non-Newtonian behavior. Such a rheology can modify the flow in a significant manner. Despite the general importance of vortical flows, only a handful of fundamental studies has addressed the effect of non-Newtonian liquid properties. Coelho and Pinho^{13,14} studied the vortex shedding behind a cylinder in cross-flow for the case of shear-thinning viscoelastic (VE) flows. They found that the shedding frequency is increased because of shear-thinning effects. Böhme *et al.*¹⁵ studied the vortex breakdown of torsionally driven cavities for shear-thinning liquids. They found that the critical Reynolds number for which the breakdown is observed is reduced; this result is attributed to the thinning nature of the fluid. Goddard and Hess¹⁶ observed that the elastic “turbulence” phenomena could appear at low Reynolds numbers considering non-Newtonian polymeric solutions. Torralba *et al.*¹⁷ observed flow vortical instabilities in a vertical tube driven by an oscillating pressure. They argued that the formation of vortices in the system was a result of the elastic properties of the liquid. For the particular case of vortex rings, the first study that addressed the influence of non-Newtonian rheology is that of Palacios-Morales and Zenit.¹⁸ They investigated the formation and evolution of vortex rings in a piston-cylinder apparatus using different shear-thinning liquids, with negligible elastic effects. They found that the vortex circulation decreases with the thinning nature of the liquid (power index n), while keeping the Reynolds number constant. More recently,¹⁹ studied the formation of vortex rings in a wormlike micellar solution generated in an oscillatory vertical pipe flow. In their case, the fluids were both shear thinning and

viscoelastic. They observed significant differences in the flow structure between Newtonian and viscoelastic fluids, attributed to the elasticity of the liquid. In particular, they studied the transition from rectilinear-laminar flow to more complex vortical flows in the pipe which were generated depending on the Deborah and Weissenberg numbers as well as the driving conditions.

In the present study, we extend our previous work¹⁸ to investigate the effect of viscoelasticity on the formation of vortex rings. In particular, we focus our study to the early stages of vortex formation and the properties of the ring in an impulsively started flow, which, to our knowledge, has not been reported in the literature. We found that the properties of the ring are modified substantially if viscoelastic effects are present. We observed the formation of “negative rings:” coherent structures with reversed spinning direction (with respect to the Newtonian case). We argue that the process that leads to the formation of these rings is similar to that observed around spheres and bubbles where “negative wakes” appear when viscoelastic effects are important.^{20–22} We believe that the study of such “simple” flows in viscoelastic media could be of value to further understand more complex non-Newtonian flow phenomena.²³ The objective of the present communication is to report these new findings. Therefore, we focus only on a limited range of parameters where the phenomena are observed. A more detailed and comprehensive study will be reported elsewhere.

The experimental setup is a classical piston-cylinder arrangement: vortex rings were generated by moving a piston which pushes a column of liquid inside a horizontal cylinder. It is described in detail in Section I of the Supplementary Material.²⁵ The Supplementary Material also provides a detailed description of the measurement uncertainties (in Sec. I) and details of the parameters considered in the PIV system (in Sec. II). The prescribed inputs for the experiment were the maximum piston velocity, U_p , and the total displacement, L . All results are shown in terms of a dimensionless time, defined as $t^* = t\bar{U}_p/D_0$, where \bar{U}_p is the mean piston velocity and D_0 is the cylinder inner diameter.

Two liquids were used: a shear thinning viscoelastic aqueous polymeric solution (VE liquid) and a Newtonian water-glycerol solution (N liquid). The VE liquid was prepared following the procedure used by Velez-Cordero *et al.*:²⁶ a small amount of a commercial polyacrilamide (0.15% wt., powder, Sigma Aldrich) was slowly dissolved into a 50%/50% wt. of water and glycerol mixture. Once the liquid was prepared, it was characterized by conducting steady shear measurements with a rheometer (Anton Paar, cone-plate, diameter of 49.97 mm, 23°, 10% constant strain). This liquid showed both shear-thinning viscosity and appearance of first normal stress difference. Details of the rheological characterization of this fluid can be found in Section III of the Supplementary Material.²⁵ The liquid was found to have a power index $n = 0.63$ and a consistency coefficient $m = 0.409 \text{ Pa s}^n$, according to a power law model. From the fit to a Maxwell-type model, a mean relaxation time, $\lambda = 0.63 \pm 0.08 \text{ s}$ was found.

The Newtonian liquid was prepared to match the Reynolds number, as close as possible, for the two flows. First, a water-glycerol mixture was prepared such that the shear viscosity, μ , had the same order of magnitude as the consistency index, m , of the VE fluid. We considered a mixture of a 20%/80% wt. of water and glycerol. Its viscosity, also measured with the rheometer, was constant $\mu = 0.073 \text{ Pa s}$, over the range of shear rates relevant to the flow, as discussed in Section III of the Supplementary Material.²⁵

Following Ref. 18, the Reynolds number was calculated considering an effective viscosity at a characteristic shear rate $\dot{\gamma} = 2U_p/D_0$, leading to

$$Re = \frac{2^{1-n} \rho U_p^{2-n} D_0^n}{m}, \quad (1)$$

where ρ is the fluid density. Using a 25 ml pichnometer, we measured $\rho_{VE} = 1125 \text{ kg/m}^3$ and $\rho_N = 1208 \text{ kg/m}^3$.

Then, a certain piston velocity was chosen for the VE fluid ($U_p = 15 \text{ cm/s}$). Considering Eq. (1), we obtained $Re_{VE} = 21.8$. From this value, the piston velocity was calculated for the Newtonian experiment considering $n = 1$ and $m = \mu$ to match $Re_N = Re_{VE}$, to result in $U_p = 9 \text{ cm/s}$. Considering these parameters, we were able to obtain $Re_N = 29.0$. Clearly, both Reynolds numbers

are closely matched. Hence, in both cases, the ratio of inertial to viscous effects is the same. Therefore, all the differences observed in the vortex formation process can be attributed to either shear thinning or viscoelastic effects.

To assess the importance of viscoelastic effects in the flow, we can construct a dimensionless parameter that compares the relaxation time, λ , to the characteristic flow time ($t_{flow} = D_0/U_p$). The ratio is the so-called Deborah number,

$$De = \frac{U_p \lambda}{D_0}. \quad (2)$$

For the VE-fluid, $De \approx 5$. Therefore, we can assert that the elastic effects in the formation of the ring in the VE liquid are significant.

Experiments were conducted for different values of the nominal stroke ratio L/D_0 , keeping the same Reynolds number. However, we opted to only focus on one particular stroke ratio: $L/D_0 = 4$. In this particular case, we observe the formation of single vortex rings for the Newtonian liquid. Therefore, we can focus only in the behavior of isolated rings. As it has been widely reported (see, for instance, Ref. 27), for smaller stroke ratios, the rings do not reach their maximum possible size; for larger ratios, on the other hand, a trailing jet is left behind the ring. Note, however, that there are no previous reports on the properties of vortex rings at such small values of the Reynolds number for Newtonian liquids.

Figure 1(a) (and corresponding Multimedia view) shows a time sequence of the velocity $\vec{v} = (u, v)$ and vorticity ω^* fields for the Newtonian case. The fluid velocity profile, u , along the vortex axis ($y = 0$) is shown for different time instants in Fig. 2(a). In this case, the ring forms in a similar manner as what has been widely reported,²⁷ for $Re \sim O(1000)$, despite the fact that the Reynolds number is smaller. For early times, $t^* < 3$, the piston is moving at a constant speed. The fluid is being expelled by the piston to form the vortex ring. The fluid velocity, u , decreases with distance from the tube, as expected. When the piston begins its deceleration, $t^* \approx 3$, the fluid velocity near the tube exit, $x = 0$, begins to decrease. The motion of the fluid beyond the exit continues, as the vortex continues to move and form. At $t^* = 4.0$, the ring separates from the nozzle, which coincides with the time piston has stopped. For this time, the fluid velocity at $x = 0$ is also very small. For later times, $t^* > 4.0$, the ring simply continues to move at constant speed and shape. The velocity profile does not evolve significantly as the ring moves forward.

In sharp contrast, for the VE fluid, significant differences are readily observable during the entire formation process as illustrated in Fig. 1(b) and its corresponding Multimedia view. First, the

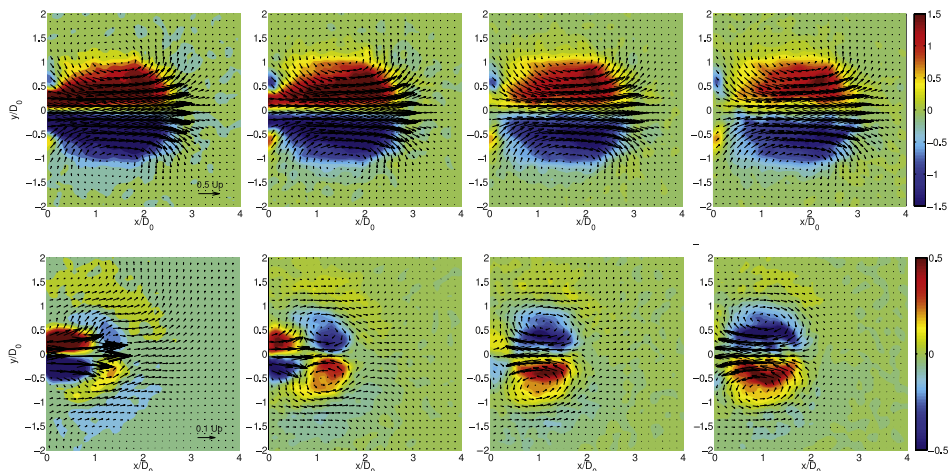


FIG. 1. Time evolution of the velocity and vorticity fields for the formation of a single vortex ring. (a) First row, N-liquid; (b) second row, VE liquid. In both cases, $t^* = [3.63, 3.85, 4.06, 4.27]$, from left to right. $L/D_0 = 4$, $Re \approx 25$, and $De \approx 5.0$ (for the VE-liquid). Vorticity is shown in dimensionless terms, $\omega^* = \omega U_p / D_0$. Note that the scale is different for both fluids. Both horizontal and vertical distances are normalized using D_0 . (Multimedia view) [URL: <http://dx.doi.org/10.1063/1.4919949.1>] [URL: <http://dx.doi.org/10.1063/1.4919949.2>]

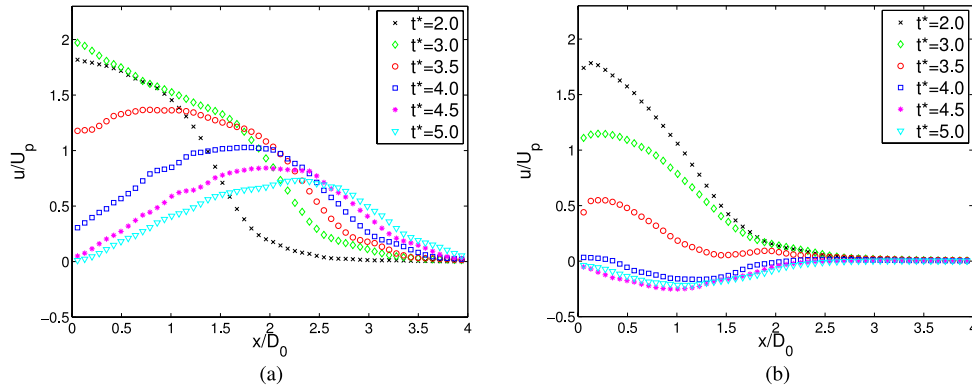


FIG. 2. Liquid velocity, u , along the axis of the vortex ring ($y = 0$) for (a) N-fluid and (b) VE-fluid. For both cases, $L/D_0 = 4$, $Re \approx 25$. Note that $x = 0$ represents the tube exit. The velocity is normalized by U_P .

size and strength (as quantified by the diameter and circulation) of the initial ring are smaller. This is in accordance with Palacios-Morales and Zenit¹⁸ who reported significant reductions in size when inelastic-shear-thinning fluids were used. However, for the liquid used here, the size of the vortex is even smaller, about half the size of the Newtonian ring. The velocity profile along the flow axis is similar to the Newtonian case for early times ($t^* < 3.0$), when the piston is moving at a constant speed. Around the time when the piston has started to slow down ($t^* \approx 3.0$), the velocity at the center decreases significantly. Also, the extent over which the fluid motion is observed outside the tube is shorter than in the Newtonian case, as observed in Fig. 2(b). The most striking difference in the formation process in between the two liquids is the appearance of a secondary vortex ring, in front of the original one. The first indication of this new structure is clearly observed in Fig. 1(b), first image on the left, corresponding to $t^* = 3.6$. Correspondingly, in Fig. 2(b), the velocity profile for approximately the same time shows a change in trend: an inflection point appears at around $x/D_0 \approx 1.5$. This new vortex ring has a rotation direction which is, in fact, opposite to that of the original ring that was forming at the exit of the tube. At approximately the time when the piston has come to a complete stop, $t^* \approx 4.0$, the “negative” vortex has fully formed and propagates in the opposite direction to that of the original fluid jet. The velocity profile clearly shows that the velocity in the flow axis is negative for $t^* > 4.0$. During the formation of the negative vortex, the size and strength of the initial ring decrease and it eventually disappears completely. It is important to note that $u \approx 0$ beyond $x/D_0 \approx 2.5$ for the VE case and $L/D_0 = 4$, i.e., the primary vortex does not travel in the x direction beyond this point.

To understand why the negative vortex forms in the VE-fluid, it is interesting to calculate the extension and shear rates of the flow. Figure 3 shows the field of extension rate in the direction of the vortex motion ($\partial u/\partial x$) and the shear rate in the perpendicular direction ($\partial u/\partial y$), for a particular time ($t^* = 3.6$), which is during the period when piston is slowing down. In the Newtonian case, there are large portions of fluid being sheared as a result of the forward-moving fluid, as shown in Fig. 3(a). At the exit of the tube ($x = 0$), a region of positive but weak extension rate is clearly identified, Fig. 3(b), which results from the fact that the fluid being issued out of the tube is at a smaller speed than that in the vortex. This feature can also be observed in Fig. 2(a). For longer distances (not shown), the extension rate becomes negative, as the fluid within the vortex “pushes” the stagnant fluid. For the VE-liquid, a significant amount of shear can be observed, above and below the ring center, as shown in Fig. 3(c), but it is confined within a smaller axial region ($0 < x/D_0 < 1$). In sharp contrast with the Newtonian case, for the VE-liquids, there is a thin region at the exit of the tube where large extension rate is observed as shown in Fig. 3(d). Most notably, right in front of the vortex, a region with negative extension rate appears. In this region, the fluid motion from the jet issuing from the tube is most likely hindered by viscoelastic effects.

As it is often discussed, when a viscoelastic fluid is sheared, an elastic stress appears in the direction perpendicular to the shearing motion.²⁸ In the case of the vortex ring formation, the elastic stress may be affecting the flow in two different manners. First, the size of the vortex ring may be

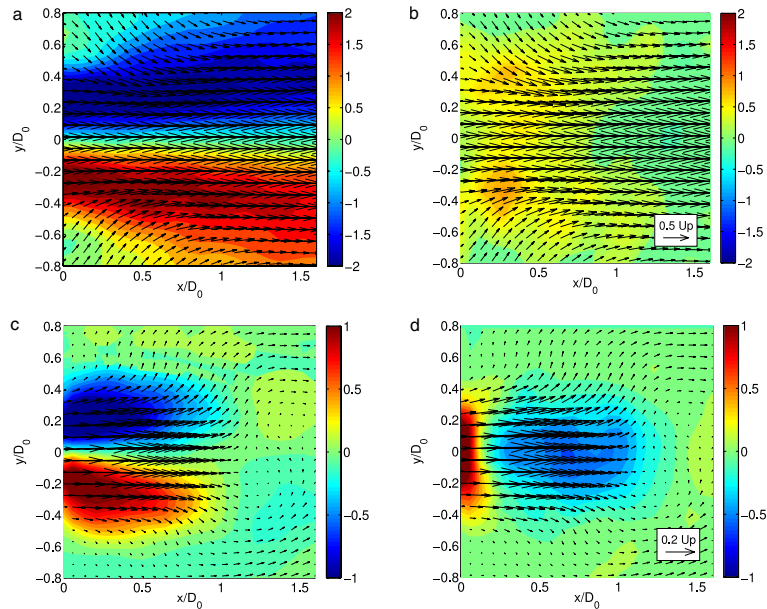


FIG. 3. Color maps of shear ($\partial u/\partial y$) and extension ($\partial u/\partial x$) rates for the N-liquid ((a) and (b)) and the ((c) and (d)) VE-liquid, respectively. For both cases, $L/D_0 = 4$ for $t^* = 3.6$. The rates are given in units of D_0/U_p .

constrained by the appearance of an elastic force at a certain distance from the tube. Such force, on the other hand, induces the appearance of a jet in the reversed direction as the fluid reacts to this additional stress. The combination of the large extension rate and the shear-induced elastic stress gives rise to the formation of a new vortical structure which has a reversed direction with respect to the initial vortex issuing from the tube, as clearly depicted in Fig. 1(b). Once the negative vortex is formed, it interacts with the initial one. Since the vorticity of the original vortex is opposite to that of the negative one, the former disappears completely in a brief time period. This process strengthens the negative vortex which continues to move backwards towards the tube. Eventually, the rotating motion is dissipated by viscous effects.

It is interesting to note that the flow field generated in these early stages of the vortex formation resembles that observed around particles and bubbles in viscoelastic media. In such a case, the fluid is also exposed to both extension and shear. The combined effect of both flow types contributes to the appearance of negative wakes, as reported by many investigations (see, for instance, Refs. 20–22). For the particular case of particles moving in viscoelastic media, Mendoza-Fuentes *et al.*²¹ studied conditions for the appearance of a negative wake in the rear of a sphere. They found that the extension rate and the strain-hardening nature of the fluid were the dominant mechanisms to observe a reversed wake. In the case of vortex ring formation, the flow is not affected by the presence of a solid interface. Therefore, we can argue that this flow may be “simpler” to assess the conditions to determine the appearance of the reversed or negative flow.

Finally, to characterize the vortex ring formation, we measured the circulation of the vortex rings in both cases. Considering the scheme proposed by Gharib *et al.*,²⁷ the circulation of the vortices is quantified by considering

$$\Gamma = \int_A \omega_z dA, \quad (3)$$

where ω_z is the fluid vorticity greater than a certain threshold value and A is the area of the flow where ring appears. In our case, we define the vortex rings as the regions where $\omega_z > 0.5 \text{ s}^{-1}$, which corresponds to 1.6% of the maximum vorticity.

Figure 4 shows the measurement of circulation as a function of time for the two liquids considered in this investigation. For the Newtonian case, Fig. 4(a), the circulation gradually increases as the piston moves, continuously increasing even after the piston has reached a steady speed. When the piston begins to slow down, the circulation begins to decrease. When the piston has stopped

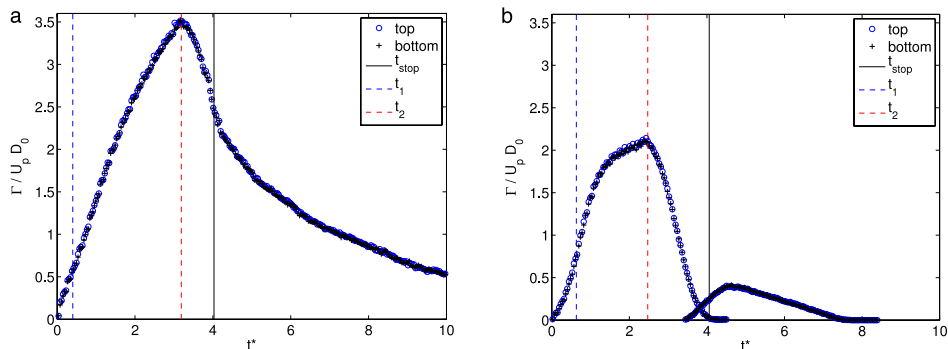


FIG. 4. Vortex ring circulation, Γ , as a function of time. (a) Newtonian liquid and (b) viscoelastic liquid. $L/D_0 = 4.0$, $Re \approx 25$, and $De = 4.9$. Measurements obtained from both top and bottom sections of the vortex rings.

completely, the circulation is observed to decrease monotonically in time. Since the Reynolds number is small, it is not possible to know if the ring has reached its saturated state. Nevertheless, the process is similar to what has been previously reported for Newtonian flows for larger Reynolds numbers.^{24,27} For the case of the VE-fluid, we observe that, in a similar manner to the Newtonian case, the circulation of the first vortex increases with time as the piston accelerates. In this case, after the piston has reached a steady velocity, the circulation grows but at a significantly smaller rate. The circulation is also smaller than that measured in the Newtonian liquid. The reduction of vortex circulation is in agreement with Palacios-Morales and Zenit,¹⁸ who measured the effect of shear thinning viscosity on the circulation of single vortex rings. However, for the case shown here, the reduction of vortex circulation is even larger than that found by Ref. 18. There are two possible causes: first, the Reynolds number in the present case is much smaller; second, the viscoelastic nature of the flow affects the circulation and vorticity conservation. Note that the value of the circulation achieved by the Newtonian vortex is similar to that measured by Ref. 24, for a flow with $Re \approx 150$; therefore, we can conclude that the viscoelasticity of the liquid is playing a more relevant role in the reduction of circulation. When the piston begins to decelerate, the vorticity begins to decrease, in a similar manner as in the Newtonian case.

Now, if the vorticity produced on the tube walls is not feeding the leading vortex ring, where is it going? We can argue that there is a fraction of the resulting stress being stored as elastic stress in the liquid. Before the piston ceases to eject fluid from the tube, as shown in Fig. 4(b), the flow reverses, as explained above, and a new vortex is produced. The negative vortex rapidly increases its circulation, as the main vortex is quickly damped. Briefly after the piston has stopped its motion completely, the negative vortex rings reached a maximum circulation (again, of opposite sign). As it moves backwards, it interacts with the tube and slowly dissipates for posterior times. It is interesting to note that the maximum circulation attained by the negative vortex is of the order of the circulation reduction of the main initial vortex (compared to the Newtonian value).

It is interesting to note that for this flow, the strong shear at the piston exit during the formation of the ring may induce the propagation of viscoelastic shear waves.²⁹ It has been reported that for the particular case of viscoelastic fluids, such waves propagate more effectively than in Newtonian liquids. Such difference in propagation may induce some of the flow features reported here.

In summary, we report the appearance of a “negative” vortex ring which results from the viscoelastic nature of the fluid in the process of forming a vortex ring. Although the appearance of flow reversal in other viscoelastic flows has been previously documented, the case of backward spinning vortices has not been reported to date. Due to the simplicity of this flow, we feel that it could serve as a benchmark test to fully understand the flow-reversal phenomena in viscoelastic flows. In this particular report, we have only reported the flow phenomena and proposed a phenomenological description of the process for a particular value of the stroke ratio. It would be interesting to further study this flow by varying the amount of elasticity of the liquid (vary the Deborah number). We expect the flow to slowly transition from Newtonian to fully viscoelastic as the Deborah number increases. It would also be interesting to increase the value of the Reynolds number, by keeping

the Deborah number constant, to observe if the condition to generate single vortex rings²⁷ is also affected by viscoelastic effects. Furthermore, it would be interesting to understand the vorticity conservation of the flow when viscoelastic effects are relevant. To our knowledge, such analysis has not been explored in detail in the specialized literature. We plan to continue exploring these ideas in the future. Gaining a deeper understanding of these issues may be relevant to further understand the nature of elastic turbulence and viscoelastic drag reduction.

We are grateful to DGAPA-UNAM for granting C. Palacios postdoctoral scholarship. The financial support to this project from PAPIIT (Grant No. IN115812) is also greatly appreciated. R. Zenit also acknowledges the support of PASPA-DGAPA-UNAM and the Fulbright Foundation during his sabbatical year at the California Institute of Technology.

- ¹ K. Shariff and A. Leonard, "Vortex rings," *Ann. Rev. Fluid Mech.* **24**, 235-279 (1992).
- ² J. H. Arakeri, D. Das, A. Krothapalli, and L. Lourenco, "Vortex ring formation at the open end of a shock tube: A particle image velocimetry study," *Phys. Fluids* **16**, 1008-1018 (2004).
- ³ O. Velasco-Fuentes, "Early observations and experiments on ring vortices," *Eur. J. Mech. B/Fluids* **43**, 166-171 (2014).
- ⁴ D. G. Akhmetov, *Vortex Rings* (Springer, 2009).
- ⁵ R. W. Whittlesey and J. O. Dabiri, "Optimal vortex formation in a self-propelled vehicle," *J. Fluid Mech.* **737**, 78-104 (2013).
- ⁶ A. A. Moslemi and P. S. Krueger, "Propulsive efficiency of a biomorphic pulsed-jet underwater vehicle," *Bioinspir. Biomim.* **5**, 036003 (2010).
- ⁷ G. K. Lucey, "Vortex ring generator: Mechanical engineering design for 100-kpsi operating pressures," ARL-TR-2096, United States Army Research Laboratory, Adelphi, MD, 2000.
- ⁸ L. Yu, W. Guo, M. Sun, and J. He, "Design and experiment of vortex rings umbrella based on finite element method," *Adv. Mater. Res.* **785-786**, 1225-1228 (2013).
- ⁹ J. O. Dabiri, S. P. Colin, and J. H. Costello, "Fast-swimming hydromedusae exploit velar kinematics to form an optimal vortex wake," *J. Exp. Biol.* **209**, 2025-2033 (2006).
- ¹⁰ E. J. Anderson and M. A. Grosenbaugh, "Jet flow in steadily swimming adult squid," *J. Exp. Biol.* **208**, 1125-1146 (2005).
- ¹¹ I. K. Bartol, P. S. Krueger, W. J. Stewart, and J. T. Thompson, "Hydrodynamics of pulsed jetting in juvenile and adult brief squid *Lolliguncula brevis*: Evidence of multiple jet 'modes' and their implications for propulsive efficiency," *J. Exp. Biol.* **212**, 1889-1903 (2009).
- ¹² M. Gharib, E. Rambod, A. Kheradvar, and D. J. Sahn, "Optimal vortex formation as an index of cardiac health," *Proc. Natl. Acad. Sci. U. S. A.* **103**, 6305-6308 (2006).
- ¹³ P. M. Coelho and F. T. Pinho, "Vortex shedding in cylinder flow of shear-thinning fluids I. Identification and demarcation of flow regimes," *J. Non-Newtonian Fluid Mech.* **110**, 143-176 (2003).
- ¹⁴ P. M. Coelho and F. T. Pinho, "Vortex shedding in cylinder flow of shear-thinning fluids II. Flow characteristics," *J. Non-Newtonian Fluid Mech.* **110**, 177-193 (2003).
- ¹⁵ G. Böhme, L. Rubart, and M. Stenger, "Vortex breakdown in shear-thinning liquids: Experiment and numerical simulation," *J. Non-Newtonian Fluid Mech.* **45**, 1-20 (1992).
- ¹⁶ C. Goddard and O. Hess, "Low Reynolds number turbulence in nonlinear Maxwell-model fluids," *Phys. Rev. E* **81**, 036310 (2010).
- ¹⁷ M. Torralba, A. A. Castrejón-Pita, G. Hernández, G. Huelsz, J. A. del Río, and J. Ortín, "Instabilities in the oscillatory flow of a complex fluid," *Phys. Rev. E* **75**, 056307 (2007).
- ¹⁸ C. Palacios-Morales and R. Zenit, "The formation of vortex rings in shear-thinning liquids," *J. Non-Newtonian Fluid Mech.* **194**, 1-13 (2013).
- ¹⁹ L. Casanellas and J. Ortín, "Vortex ring formation in oscillatory pipe flow of wormlike micellar solutions," *J. Rheol.* **58**, 149-181 (2014).
- ²⁰ E. Soto, C. Goujon, R. Zenit, and O. Manero, "A study of velocity discontinuity for single air bubbles rising in an associative polymer," *Phys. Fluids* **18**, 121510 (2006).
- ²¹ A. J. Mendoza-Fuentes, R. Montiel, R. Zenit, and O. Manero, "On the flow of associative polymers past a sphere: Evaluation of negative wake criteria," *Phys. Fluids* **21**, 033104 (2009).
- ²² J. R. Herrera-Velarde, R. Zenit, D. Chahata, and B. Mena, "The flow of non-Newtonian fluids around bubbles and its connection to the jump discontinuity," *J. Non-Newtonian Fluid Mech.* **111**, 199-209 (2003).
- ²³ M. D. Graham, "Drag reduction and the dynamics of turbulence in simple and complex fluids," *Phys. Fluids* **26**, 101301 (2014).
- ²⁴ C. Palacios-Morales and R. Zenit, "Vortex ring formation for low Re numbers," *Acta Mech.* **224**, 383-397 (2013).
- ²⁵ See supplementary material at <http://dx.doi.org/10.1063/1.4919949> for details about the experimental setup (Section I), the PIV system (Section II) and the rheological characterization of the viscoelastic fluid (Section III). The parameters to obtain the velocity fields with the PIV system are listed. Fits for both the shear viscosity and first normal stress difference are shown to obtain the power index, n , the constancy, m , and the relaxation time, λ , of the viscoelastic fluid.
- ²⁶ J. R. Velez-Cordero, D. Samano, and R. Zenit, "Study of the properties of bubbly flows in Boger-type fluids," *J. Non-Newtonian Fluid Mech.* **175-176**, 1-9 (2012).
- ²⁷ M. Gharib, E. Rambod, and K. Shariff, "A universal time scale for vortex ring formation," *J. Fluid Mech.* **360**, 121-140 (1998).
- ²⁸ H. A. Barnes, J. F. Hutton, and K. Walters, *An Introduction to Rheology* (Elsevier, 1989).
- ²⁹ P. P. Niiler and A. C. Pipkin, "Finite amplitude shear waves in some non-Newtonian fluids," *Int. J. Eng. Sci.* **2**, 305-313 (1964).